C. R. Mecanique 339 (2011) 719–726

Contents lists available at ScienceDirect

Comptes Rendus Mecanique

www.sciencedirect.com

Critical state notion and microstructural considerations in clays

Mahdia Hattab

Laboratoire d'Etude des Microstructures et de Mécanique des Matériaux, UMR CNRS 7239, Université Paul Verlaine, île du Saulcy, 57045 Metz cedex 1, France

ARTICLE INFO

Article history:
Received 3 April 2011
Accepted after revision 21 July 2011
Available online 27 August 2011

Keywords:
Soils
Critical state line
Shear mechanism
Fabric/structure
Microscopy
Kaolinite
Triaxial tests

ABSTRACT

The aim of the experimental study was to identify the local deformation properties in a clayey material which can be activated at the macroscopic ultimate state known by critical state. The approach consists of an extensive study, based on a Scanning Electron Microscope (SEM) picture analysis, of the orientation of the clay particles characterized in the last stages of triaxial loading.

1. Introduction

The critical state notion was stated by Roscoe et al. [1] for describing the state in large deformations of an idealized soil material. The latter material flows as a frictional fluid, after being continuously sheared. Many authors develop "phenomenological" constitutive models based on the critical state concept, like, for example, the elasto-plastic Cam clay models [2–4], or more sophisticated models such as models of Dafalias and Herrmann [5] and Hujeux [6]. These approaches consist of predicting the behavior at the global (macroscopic) level of the specimen, using the principles of the mechanics of continuous media in the formal framework of elasto-plasticity. The triaxial test constitutes, in this way, a basic means for experimental investigation. Numerous test results highlighted the existence of the critical state that is regarded as an ultimate state toward which all triaxial paths (deviatoric path, volumetric constant path, and effective radial constant path for instance) tend. The latter phenomenon is also defined by Biarez and Hicher [7] as the perfect plastic state.

Microscopically, a few works using different experimental methods investigated the microstructure change of clayey materials during triaxial shear loading (see for instance following works [8–11]). On kaolinite specimens, Morgenstern and Tchalenko [12], using polarized light microscopy, showed a strong orientation of particles in the direction of movement during a direct shear test. Hicher et al. [13] used scanning and transmission electron micrographs to study the changes in the microfabric of saturated kaolin and bentonite specimens after drained triaxial tests: they observed the creation of structural anisotropy during loading and concluded that the mechanical behavior is largely dependent on the changes that occur at the particle level. More recently Hattab and Fleureau [14,15] quantify this anisotropy variation on kaolin clay establishing the relation between particle orientation variations during triaxial path.

In the present experimental study we try to identify the local mechanism, which can develop at microscopic scale, at the specific state of the macroscopic behavior where the triaxial path tends towards ultimate critical state. The tests were

E-mail address: hattab@univ-metz.fr.

1631-0721/$ – see front matter
doi:10.1016/j.crme.2011.07.007

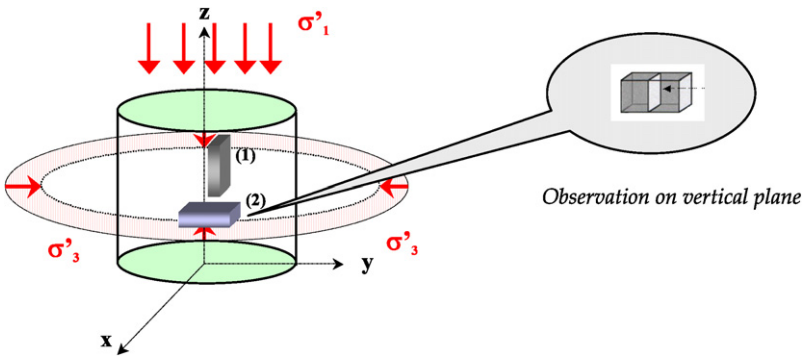

Fig. 1. Samples for SEM observations and stress state.

performed on the remoulded saturated clay specimens (kaolinite), at normally consolidated and overconsolidated conditions. A specific set up of the samples is used in order to maintain the homogeneity of their deformations during the loading.

2. Material properties and experimental set up

2.1. Material properties

Tests were performed on specimens of "kaolin P300", which is industrial clay containing about 95% of pure kaolinite. The liquid and plastic limits are $w_L = 40\%$ and $w_P = 20\%$ respectively, the unit weight of solid grains corresponds to $\gamma_s/\gamma_w = 2.65$.

2.2. Experimental set-up for mechanical tests

The experimental system performed for the mechanical tests consisted of a triaxial cell connected to three pressure-volume controllers and a microcomputer for control and data acquisition. The controllers insure the control of the radial stress σ_3, of the axial stress σ_1 (generated by the displacement of a jack in the bottom part of the cell) and of the back pressure. They also allow the measurement of changes of volume, force and axial displacement. Triaxial tests were carried out on saturated clay samples, the first step consisting in checking the quality of the saturation by following Skempton's coefficient B, where $B = \Delta U/\Delta\sigma_3$ approaching the 100%.

Specimens were prepared from clay slurry mixed with a water content of twice the liquid limit. The slurry was deposited and then consolidated in several steps at a vertical stress of 120 kPa. Then cylindrical specimens were cut, so that the length $H = 35$ mm and diameter $D = 35$ mm, and installed in the triaxial cell provided with an anti-frictional system allowing drainage at the two extremities. The anti-frictional device was made of two circular smooth plates lubricated by means of a grease and latex layers "sandwich". This kind of procedure appears as necessary to maintaining the homogeneity of the sample to large strains, by significantly reducing friction at the sample ends (see works [16–18]).

Normally consolidated and overconsolidated tests (with a triaxial loading at $\sigma'_3 = \text{constant}$) were performed. The effective consolidation stresses $p'_{c,0}$ for normally consolidated tests were 700 kPa, 1000 kPa, and 1400 kPa, for tests noted NC700, NC1000, and NC1400 respectively. The effective consolidation stress for overconsolidated tests with an OCR of 1.4 and 9.33, was $p'_{c,0} = 1400$ kPa. All Tests were stopped for microstructural investigations when the axial strain reached $\varepsilon_1 = 25\%$. Specimens were thus recovered from the cell after triaxial unloading, by first removing the deviatoric stress, then the isotropic stress under undrained conditions.

2.3. Analysis for microstructural observations

Further explanations of test procedure and microstructural identification (that we did not detail here) can be found in Hattab et al. [19]. The method consists in analyzing, starting from observations in the SEM, the orientation of the clay particles through two planes (a horizontal plane and a vertical plane) of small samples cut in the specimen. After mechanical loading, two small parallelepipedic samples were extracted from the specimen (Fig. 1), and precisely marked according to their orientation with respect to the direction of the principal stresses σ_1 and σ_3. In order to keep the fabric in suitable conditions inside the material, we first froze the samples in liquid nitrogen and then freeze-dryied them afterwards following the method advocated by Delage and Pellerin [20]. The planes for observation were then obtained by fracturing these frozen samples. The SEM pictures were then taken at various observation points on the observation plane. A semi-automatic specific method, using image processing, was developed to identify the orientation of clay particles with respect to the horizontal plane (orientation 0° is attributed to the plane perpendicular to the axial loading).

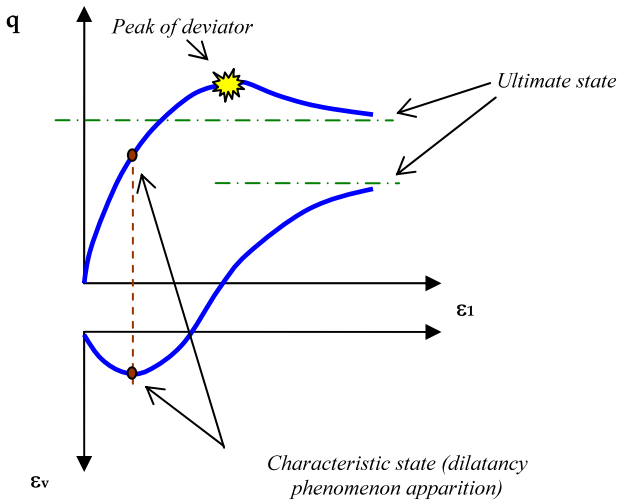

Fig. 2. Typical triaxial behavior (*at constant* σ'_3) of overconsolidated saturated clays.

3. Critical state concept

3.1. Basic notions for phenomenological experimental approach

The application in soils of an effective stress tensor $\underline{\underline{\sigma}}'$ can be divided into two parts: the deviatoric part $q \cdot \underline{\underline{d}}$ and the isotropic part $p' \cdot \underline{\underline{I}}$, such as:

$$\underline{\underline{\sigma}}' = q \cdot \underline{\underline{d}} + p' \cdot \underline{\underline{I}} \tag{1}$$

In the special case of an axisymmetric compression test, the isotropic part of the stress tensor is defined by $p' = (\sigma'_1 + 2\sigma'_3)/3$ and the deviatoric part by $q = \sigma'_1 - \sigma'_3 \cdot \sigma'_1$ is the major principal effective stress, and σ'_3 is the minor principal effective stress.

Following σ'_3 *constant* triaxial path on saturated clays, two possible behaviors can be exhibited [21]:

- A contactancy behavior for a normally consolidated and slightly overconsolidated (OCR < 2) clays. The curves show a gradual evolution of both volumetric strain ε_v and the deviator q, with respect to axial strain ε_1, toward an ultimate state (plateau).
- A dilatancy behavior for highly overconsolidated clays (OCR > 2), see the experimental extensive study on dilating phenomenon of Hattab and Hicher [22]. The behavior here is characterized by a volumetric strain curve, with respect to the axial strain, exhibiting a contractancy phenomenon (decrease of the specimen volume) in the first stages of the loading, followed by a dilatancy (increase of the specimen volume). The point of the transition between the two behaviors was defined by Luong [23] as the *characteristic state*. The deviator with respect to ε_1 exhibits a pick of maximum strength before tending, with ε_v, to an ultimate state (see illustration in Fig. 2).

3.2. Critical state concept [1,4]

Numerous tests performed on soil samples, following different triaxial loading paths (see the works collected by Biarez and Hicher [7]), have shown the existence of an ultimate state called by Roscoe et al. [1] "critical state". This ultimate state, toward which all triaxial paths lead (see *constant* p' paths in Fig. 3 for instance) and characterized by an increment of volumetric strain $d\varepsilon_v = 0$, represents a curve in (e, p', q) space (Fig. 4). Its projection on $(p'–q)$ plane is a line of M slope, and the projection on $(e– \log p')$ plane is a line (*CSL, critical state line*) which is parallel to the isotropic loading path c_c (*ISL, isotropic state line*). e represents the void ratio.

Roscoe et al. [1] introduce the notion of critical void ratio (e_c), which is the void ratio corresponding to the consolidation stress p'_{ic}, that permits to deduce on the CSL line the p'_{crit} parameter. Hence, we obtained the linear relation of critical state expressed by (2) in $(\log p', e)$ plane, and by the Mohr–Coulomb type law (3) in the stresses plane (p', q). p'_α is equal to 1 kPa, and M parameter is related to the internal friction angle ϕ'_{crit} by the following relation: $\phi'_{crit} = \arcsin(3M/(6+M))$.

$$e_c = e_{pp} - C_c \log\left(\frac{p'_{crit}}{p'_\alpha}\right) \tag{2}$$

$$q_{crit} = M p'_{crit} \tag{3}$$

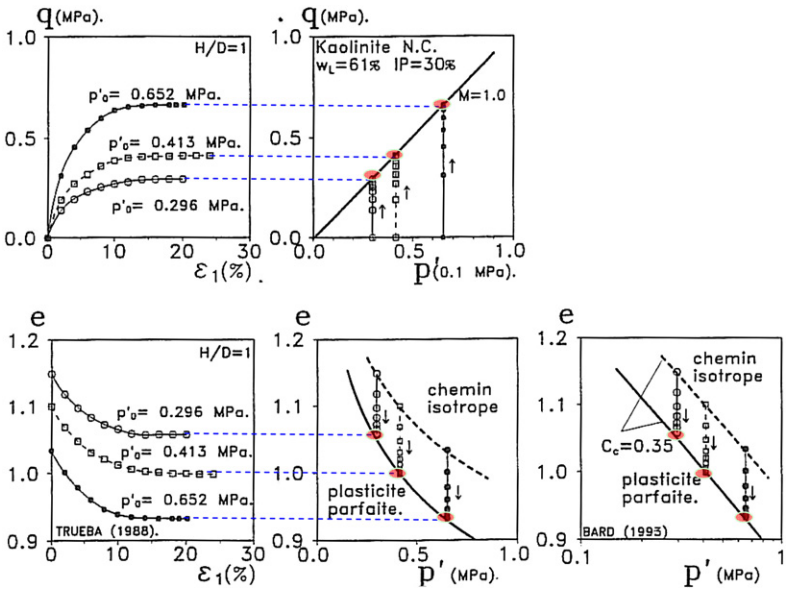

Fig. 3. Triaxial behavior of clays on purely deviatoric paths [7].

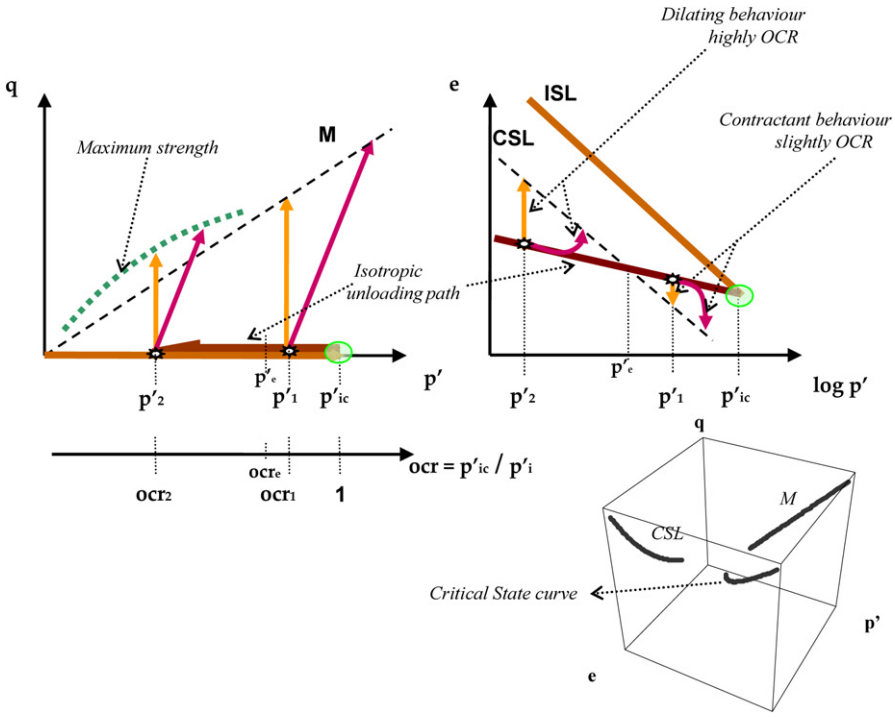

Fig. 4. Triaxial behavior of clays illustration on *purely deviatoric* and *constant* σ_3' paths and critical state concept.

3.3. Critical state identification on kaolin P300

The triaxial drained behavior of saturated remoulded clays is now well known (in particular that of kaolin P300, which was the subject of numerous studies in the past) and has been conceptualized in particular by Biarez and Hicher [7]. As it can be shown in Fig. 5, tests carried out on Kaolin P300 highlight the contractant behavior of normally consolidated or weakly overconsolidated (OCR $<$ 2) clays, and the dilatant behavior of highly overconsolidated clays (OCR $>$ 2), the dilatancy appearing after the first phase of contractancy. Afterwards, all paths lead progressively towards the ultimate critical state, defined by M slope of 1.02 on (p'–q) plane (which corresponds to an internal friction angle of 26°) and PP slope of 0.191 on ($\log p'$–e) plane.

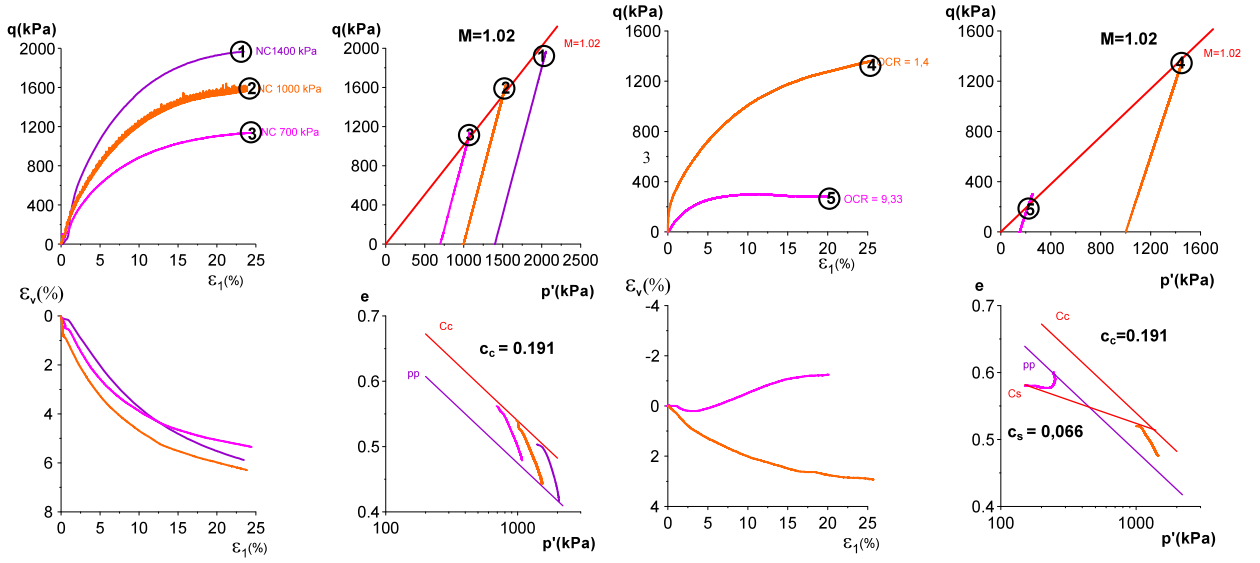

a) normally consolidated clay NC1400 – NC1000 – NC700

b) overconsolidated clay with p'_{ic}=1400 kPa ocr=1.4 – ocr=9.33

Fig. 5. Triaxial behavior of saturated remoulded kaolin P300 [24].

We tried in what follow to understand how the microstructural state of the clay, especially the orientation of clay particles, can explain this ultimate state (critical state) obtained at macroscopic scale. Microscopic observations were thus performed at the last stages of constant σ'_3 paths (Fig. 5), on normally consolidated (points 1, 2, 3 for respectively NC1400, NC1000 and NC700 paths) and overconsolidated remoulded saturated clay (points 4 and 5 for respectively OCR1.4 and OCR9.33 paths).

4. Orientation clay particles at macroscopic ultimate state

Hattab and Fleureau [13,14] demonstrated that a rotation mechanism of particles towards preferential planes is occurred during the triaxial path which seems to be directly linked to the deviatoric part of stress tensor variation. On the other hand, the isotropic part of stress tensor tends to induce a depolarization mechanism defined as an isotropic microstructural tendency. The approach proposed here consists in identifying the orientation of the kaolinite particles (by SEM images analysis) at the last stages of the triaxial loading, considering the specimen behavior close to the critical state. In this paper only some images have been presented where we can see the mechanisms observed on most of the SEM photos. More quantitative analyses are represented by the curves of percentage of oriented particles (noted $\%P$) versus the angle of orientation (denoted by θ and identified with respect to the horizontal plane). Those curves were deduced from different SEM images taken at several points on the observed plane, and then, can well translate the phenomena which locally appear.

4.1. Orientation of the particles in the last stages of triaxial paths

The SEM observations were carried out where the stress level was close to critical state, that corresponds to axial deformation of $\varepsilon_1 = 25\%$ (see points 1, 2, 3, 4, and 5 of Fig. 5).

Most of images taken in different points on the observed planes (especially vertical planes where mechanisms are well observed) highlight preferential orientations of groups of particles organized with a face to face association (see the example of NC1000 specimen presented in Fig. 6). The preferential orientations seem to be always between 30° and 45° with respect to the horizontal. On the other hand, thresholding performed on SEM photos in the oriented particles area, seems to suggest that this microstructure organization is done with a denser aspect in the case of normally consolidated clay. The examples presented in Fig. 7, on which the void is represented by black zones, show the difference obtained between a normally consolidated clay (case of NC1000) and overconsolidated (case of OCR1.4) after triaxial loading. Some open cracks can sometimes appear as well as a very strong orientation of the particles, which seems to be parallel to the cracks' planes. It is the case of the slightly over consolidated clay OCR1.4 represented in Fig. 8, which exhibits in the cracks zones a less dense structure as Fig. 7 clearly shows. This evolution toward a very marked structural anisotropy at the end of loading has been also observed by Hicher et al. [13] on two different types of clay, the kaolinite studied here and a bentonite. The angular distribution rose diagram of the vertical planes (Fig. 8) can be analyzed as orientation curves in the $\%P$–θ plane defined above. The latter representation allows us to superimpose the different curves in order to compare them (Fig. 9). The depolarization line designates the structural isotropy of a fictional material, and *principal orientation mode* represents

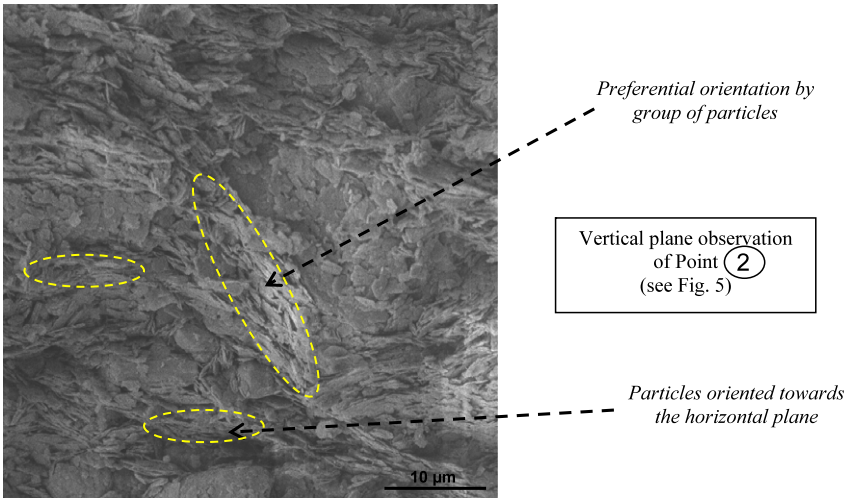

Fig. 6. Microfabric of NC1000 specimen.

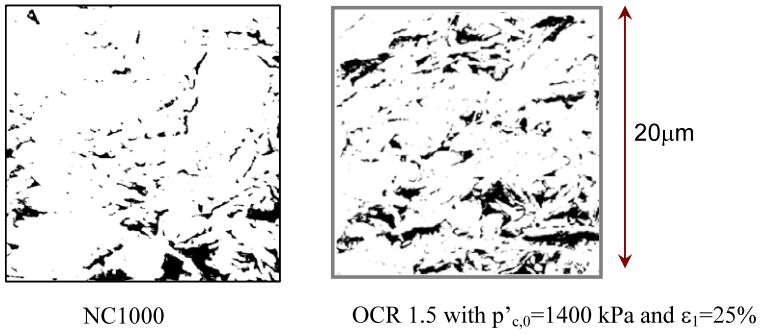

Fig. 7. Thresholding of SEM images taken after triaxial loading on point 2, and 4 of Fig. 5.

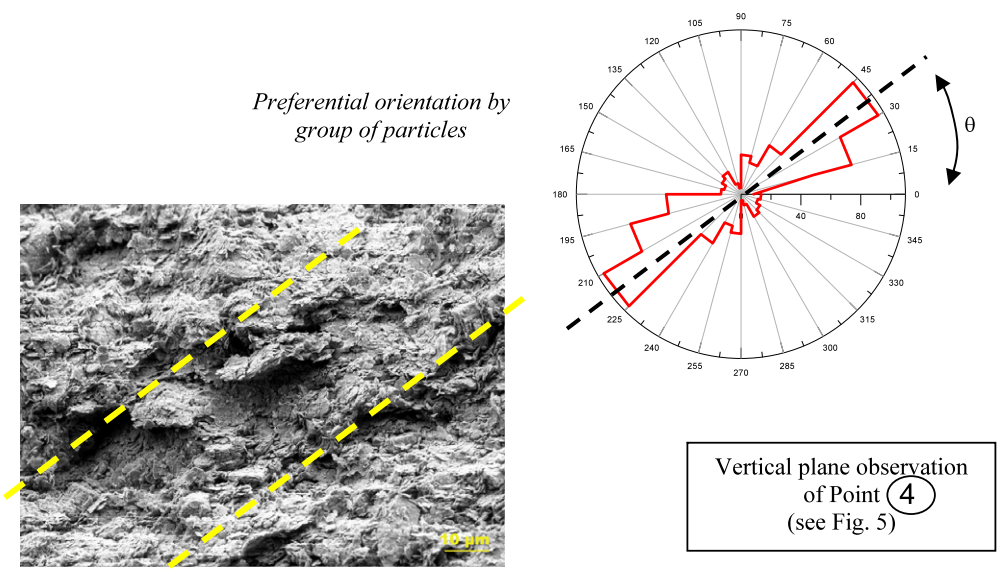

Fig. 8. Particle orientation and angular distribution of rose diagram of OCR1.4 specimen.

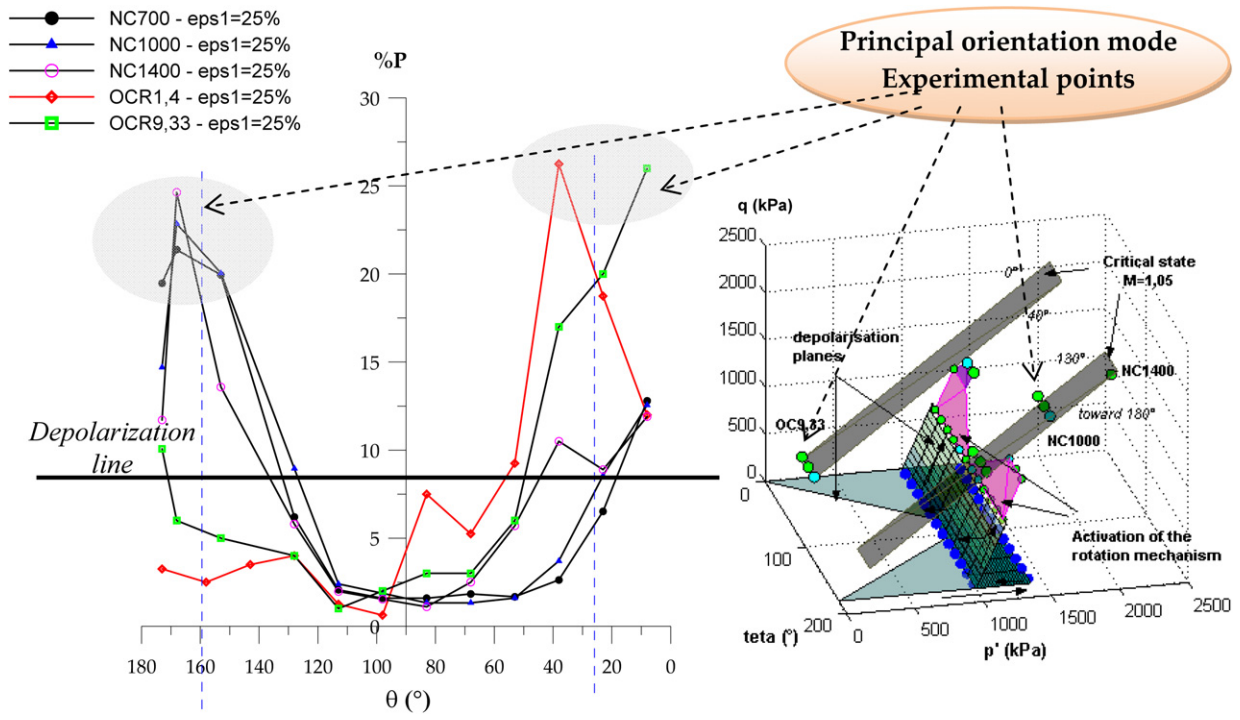

Fig. 9. Microstructure at the critical state.

high percentage of orientation ($\%P$) (around 20%): for instance, by U shape of a given curve, we obtain two principal modes of orientation which clearly identify structural anisotropy.

The results represented in Fig. 9, show that the isotropic consolidation stresses value does not affect the obtained *principal orientations*; those are located mainly toward 40° and toward 25° (with respect to the horizontal). On the other hand, all curves exhibit a significant presence of oriented particles arranged following the horizontal plane. Fig. 6 exhibits clearly this orientation. Therefore at the critical state, the consolidation stress does not seem to influence the microstructural organization of the clay.

In the $(q–p'–\theta)$ space (Fig. 9) the *principal orientations* are related to the macroscopic stresses, the deviator and the effective mean stress. Critical state is here defined by $q/p' = M = 1.02$, which are two symmetrical planes, limited by the possible preferential orientations for ultimate state (i.e. [0°–40°] and [180°–130°]) identified in this study. Consequently, even if at the macroscopic level, and in agreement with critical state concept, no localization was observed (cause of the set up of the sample), this study shows that the material is structured into different zones where particles can associate themselves according two possible orientations: one in zones that can be defined as active (40°), the other in steady zone oriented towards 0°.

This finding is mainly based on the results of particle orientation curves presented in Fig. 9, that translate in quantitative form the SEM pictures analysis. Each curve represents a global result of numerous SEM photos taken in a given condition of triaxial loading.

On the other hand, the observations conducted on all analyzed SEM photos show that preferential orientations are formed by groups associated particles and not particles individually oriented. The pictures 6 and 8 illustrate well this observation. A conceptual scheme can thus be proposed (Fig. 10) for an idealized microstructure representation available in the last stages of triaxial loading. This scheme may be that of elementary volume, where slip mechanisms can be activated.

5. Conclusion

This research proposes an explanation of the link between the critical ultimate state, obtained at the macroscopic global level of the sample, and the microstructural state of a kaolinite. The approach consists in studying the orientation of clay particles from the scanning electron microscope observations.

This present study shows clearly that the isotropic consolidation stresses in a triaxial loading does not affect the *principal orientations* obtained at the last stages of loading. Therefore, at the ultimate critical state, the material seems to be structured into different zones where particles can associate themselves according two possible orientations: one in zones that can be defined as active (40°) the other in steady zone oriented towards 0°. A conceptual scheme is proposed for an idealized microstructure representation, which can represent the elementary volume, where slip mechanisms can be activated at the ultimate critical state.

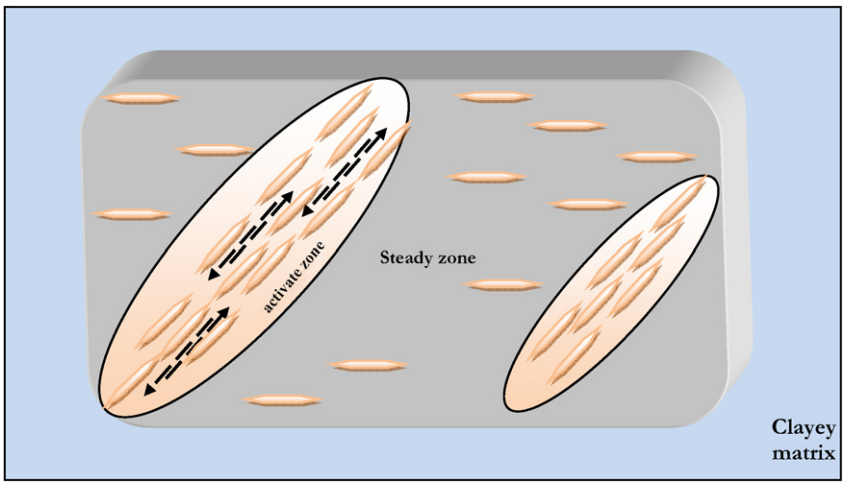

Fig. 10. Conceptual model for local mechanism at critical state.

Acknowledgement

The author wants to thank Pr. Jean-Marie Fleureau and Pr. Pierre-Yves Hicher for fruitful discussions.

References

[1] K.H. Roscoe, A.N. Schofield, C.P. Wroth, On the yielding of soils, Géotechnique 8 (1) (1958) 22–53.
[2] K.H. Roscoe, A.N. Schofield, Mechanical behavior of an idealised 'wet' clay, in: Proc. 2nd Eur. Conf. SMFE, Wiesbaden, vol. 1, 1963, pp. 47–54.
[3] K.H. Roscoe, J.B. Burland, On the generalised stress-strain behavior of 'wet' clay, in: J. Heyman, F.A. Leckie (Eds.), Engineering Plasticity, Cambridge University Press, 1968, pp. 535–609.
[4] A.N. Schofield, C.P. Wroth, Critical State Soil Mechanics, McGraw-Hill, New York, 1968.
[5] Y.F. Dafalias, L.R. Herrmann, Bounding surface formulation of soil plasticity, in: G.N. Pande, O.C. Zienkiewicz (Eds.), Soil Mechanics – Transient and Cyclic Loads, Wiley & Sons, New York, 1982, pp. 253–311.
[6] J.-C. Hujeux, Une loi de comportement pour le chargement cyclique des sols, in: V. Davidovici (Ed.), Génie Parasismique, Presses ENPC, 1985, pp. 278–302.
[7] J. Biarez, P.-Y. Hicher, Elementary Mechanics of Soils Behavior – Saturated Remoulded Soils, Balkema, Rotterdam–Brookfield, 1994.
[8] R.T. Martin, C.C. Ladd, Fabric of consolidated kaolinite, Clays and Clay Minerals 23 (1975) 17–25.
[9] X. Bai, P. Smart, Changement de la microstructure de la kaolinite soumise à un chargement triaxial non drainé, Géotechnique 47 (5) (1997) 1009–1017.
[10] R. Pusch, Microstructural changes in soft quick clay at failure, Canadian Geotechnical Journal 7 (1997) 1–7.
[11] P. Dudoignon, A. Pantet, L. Carrara, B. Velde, Mesure micro-macro de l'arrangement des particules de kaolinite sous chargement triaxial, Géotechnique 51 (6) (2001) 493–499.
[12] N.R. Morgenstern, J.S. Tchalenko, Microscopic structures in kaolin subjected in direct shear, Géotechnique 17 (1967) 309–328.
[13] P.-Y. Hicher, H. Wahyudi, D. Tessier, Microstructural analysis of inherent and induced anisotropy in clay, Mechanics of Cohesive-Frictional Materials 5 (2000) 341–371.
[14] M. Hattab, J.-M. Fleureau, Experimental analysis of kaolinite particle orientation during triaxial path, International Journal for Numerical and Analytical Methods in Geomechanics 35 (5) (2011) 947–968.
[15] M. Hattab, J.-M. Fleureau, Experimental study of kaolin particle orientation mechanism, Géotechnique 60 (5) (2010) 323–331.
[16] P.-Y. Hicher, Comportement mécanique des argiles saturées sur divers chemins de sollicitations monotones et cycliques application à une modélisation élastoplastique et viscoplastique, Thèse de doctorat d'état des sciences physiques, Paris 6, 1985.
[17] P.V. Lade, J. Tsai, Effects of localization in triaxial tests on clays, in: Proc. ICSMFE, San Francisco, vol. 1, 1985, pp. 549–552.
[18] J.D. Frost, C. Yang, Effect of end platens on microstructure evolution in dilatant specimens, Soils and Foundations 43 (4) (2003) 1–11.
[19] M. Hattab, S. Bouziri-Adrouche, J.-M. Fleureau, Evolution de la microtexture d'une matrice kaolinitique sur chemin triaxial axisymetrique, Canadian Geotechnical Journal 47 (1) (2010) 34–48.
[20] P. Delage, M. Pellerin, Influence de la lyophilisation sur la structure d'une argile sensible du Quebec, Clay Minerals 19 (1984) 151–160.
[21] D.J. Henkel, The effect of overconsolidation on the behavior of clays during shear, Géotechnique 6 (1956) 139–150.
[22] M. Hattab, P.-Y. Hicher, Dilating behavior of overconsolidated clay, Soils and Foundations 44 (4) (2004) 27–40.
[23] M.P. Luong, Etat caractéristique du sol, C. R. Acad. Sci. Paris 287 (15) (1978) 305–307.
[24] Bouziri, Etude des mécanismes de déformation dans les argiles surconsolidées, Thèse de doctorat de l'Ecole Centrale Paris, Chatenay-Malabry, 2007.